engineering proceedings

MDPI

Proceeding Paper

Microwave Radar Imaging as a Tool for Medical Diagnostics †

Antonio Cuccaro [1], Angela Dell'Aversano [2], Bruno Basile [3] and Raffaele Solimene [2,4,]*

[1] Department of Informatics, Modeling, Electronics and Systems Engineering (DIMES), University of Calabria, 87036 Rende, Italy; antonio.cuccaro@unical.it
[2] Dipartimento di Ingegneria, Università degli Studi della Campania Luigi Vanvitelli, 81031 Aversa, Italy; angela.dellaversano@gmail.com
[3] TTC Medical, 80013 Casalnuovo di Napoli, Italy; bruno.basile@temnography.com
[4] Consorzio Nazionale Interuniversitario per le Telecomunicazioni-CNIT, 43124 Parma, Italy
* Correspondence: raffaele.solimene@unicampania.it

† Presented at the 4th International Electronic Conference on Applied Sciences, 27 October–10 November 2023; Available online: https://asec2023.sciforum.net/.

Abstract: Microwave radar imaging is a diagnostic technique that is receiving significant attention in the research community for the striking advantages it may potentially offer. Nonetheless, diagnosis via microwave radar imaging is extremely difficult due to theoretical as well as practical reasons. In this contribution, in particular, we focus on the need to take frequency dispersion effects and the antenna's frequency response into account. In more detail, we propose an imaging algorithm that works by completely ignoring the tissue frequency behaviour as well as the antenna's response. The numerical results obtained via a full-wave electromagnetic solver for a simplified breast layout confirm the potential of the proposed approach.

Keywords: microwave radar imaging; medical diagnostics; breast cancer detection

check for updates

Citation: Cuccaro, A.; Dell'Aversano, A.; Basile, B.; Solimene, R. Microwave Radar Imaging as a Tool for Medical Diagnostics. *Eng. Proc.* **2023**, *56*, 303. https://doi.org/10.3390/ASEC2023-16522

Academic Editor: Nunzio Cennamo

Published: 1 December 2023

1. Introduction

Breast cancer is the most frequent cause of death due to cancer among female patients [1,2]. In this framework, early detection is crucial since the survival rate depends on the stage the disease is when it is diagnosed [3,4]. That is why, scholars continue to focus on the improvement of currently employed diagnostic methods as well as on the development of new imaging modalities that can supplement the first ones. In the last decades, microwave breast imaging (MBI) was the subject of a great deal of research since it does not rely on ionizing radiations, does not require breast compression and the related technology is relatively cheap [5]. Moreover, MBI is sensitive to the dielectric contrast between the normal and diseased tissues, which in turn is generally higher than the radiographic density contrast [6]. Results show in literature suggest that MBI can actually be used for breast cancer [7–9].

Many algorithms for MBI have been developed [10] till now. Some of them directly reconstruct the 3D scenario under test, others, instead, reconstruct the scene as a collections of 2D problems (sliced approach), which reduces the imaging algorithm complexity [11]. In general, microwave breast imaging entails solving a non-linear ill-posed inverse scattering problem which is much more difficult than for X-ray tomography since diffraction phenomena cannot be ignored. Non-linear inversions are cast as an optimization problem where the misfit between the measured and the model data is generally minimized by iterative algorithms [12]. Accordingly, the related reconstruction procedures are computationally heavy [13] and can be trapped in some false solutions [14]. Assuming a linear scattering model simplifies the imaging problem and leads to the so-called radar imaging approach [15]. In this case, the imaging is robust against noise and uncertainties and computationally effective, though the corresponding images appear more like hot maps where strong inhomogeneities are detected. Eventually, the radar imaging allows for only the detection and the localization of targets which have a strong dielectric contrast with respect to the surrounding background tissues. The beam-forming (BF) algorithm is for sure the most popular MBI method. Basically, for each pixel in the scene, the received signals are properly time-shifting and the summed so to focus at the considered pixel belonging to the spatial area to be imaged [16]. Different variant of BF have been proposed in literature [17–19]. A detailed analytical study on the achievable performance by BF methods has been reported in [20], where the working frequency and the number of spatial data points, was highlighted.

Even under the simplified framework of the radar approach, to success in the imaging a number of issues need to be properly dealt with. For example, before imaging, data must be pre-processed in order to reduce the clutter due to the antenna's internal reflection, the skin interface and other non-tumor breast tissues [21]. Another important issue to face is the frequency dispersion of breast tissues. This is particularly true for wide band imaging methods and because the tissues generally vary from patient to patient. Accordingly, during imaging procedure the breast is actually unknown. At this juncture, since the antenna works near the breast, even its behaviour frequency response becomes not predictable and unknown [22,23].

In this contribution, we assume that the background measurement is available so that the focus on the issue related to the tissue frequency dispersion and antenna's frequency response. It is clear that these two issues entail performance degradation in standard BF methods. This is mainly because standard BF "coherently" combine data collected at different frequencies. Indeed, frequency dispersion and unknown antenna's response lead to error while devising the delay set to be used in the beam-forming procedure. To mitigate such a drawback, the same incoherent imaging algorithms used in [22,24,25] are adopted for 3D breast microwave imaging. In [26], experiments confirmed the validity of incoherent approach in medical imaging. In particular, a prototype for breast cancer imaging [23] and a Subcranial Encephalic Temnograph (TES) system for stroke detection are adopted. The main features of incoherent approach are summarized in Section 3 while a complete analysis can be found in [20,25]. Differently from [26,27], we perform a numerical analysis in a multistatic configuration by adopting a conformal array to breast model. Moreover, a 3D reconstruction procedure is employed (instead of the sliced approach used in [27]). The results shown that the performance are satisfactory although, during the imaging stage, the antenna's frequency response is completely ignored and the tissue variations with frequency are not accounted for.

2. Measurement Configuration Description

The idea is to deploy N antennas over a hemispherical cup that surrounds the breast under test as sketched in Figure 1a,b. Denote as $\underline{r}_{on}$, for $n = 1, 2, \cdots, N$, the positions of the corresponding antenna phase centers. The cup solution offers a number of advantages. First, the system has not sliding antennas. This makes the acquisition quicker and there are no mechanical transients to wait for before staring data collection. Second, the reciprocal position between antennas with respect to the breast are fixed and precisely known. This is because when the breast is inserted in the cup the latter shapes the breast so to conform to the cap surface. Of course, from an anatomical point of view, there are different breasts size and this this requires different cups. Here, for instance the cup has internal diameter of 100 mm. Finally, the material of the cup can be considered as further design parameter. Indeed, it could be chosen in order to improve the coupling between the antenna and the breast. In particular, acrylonitrile butadiene styrene (ABS) material is used and the cup has N = 20 empty housings where to place the antennas (Figure 1c). This, along with a proper design of the antennas, allows to avoid the use of the coupling medium, which is, instead, commonly employed in microwave breast imaging systems. As to the antennas, we consider printed slot dipoles built on FR4 substrate of thickness 0.8 mm (see Figure 1c). More specifically, to reduce the physical dimensions of the antenna, the breast loading effect is exploited. This is achievable if during the design procedure, the antenna is placed in direct contact with the breast. In particular, since in actual breasts the first two layers are skin and fat, a simplified numerical phantom consisting of only these tissues is considered. Also, for antenna design within [4, 6] GHz frequency band, the skin and fat layers are considered planar and having thicknesses 1.5 mm and 50 mm, respectively. This speeds up the antenna optimization process while using a full-wave electromagnetic solvers. Both tissues are modeled employing the four-poles Cole-Cole models reported in four-poles Cole-Cole models reported in [28]. At central frequency (i.e., 5 GHz in our case), the electromagnetic properties of skin and fat layer are ($\epsilon_r = 35.78$, $\sigma = 3.06$ S/m) and ($\epsilon_r = 5.08$, $\sigma = 0.24$ S/m), respectively. As discussed in Section 1, these represent nominal values that can differ from the actual ones.

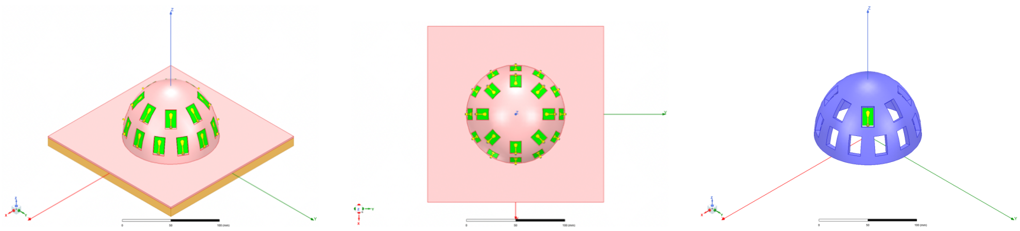

(**a**) (**b**) (**c**)

Figure 1. Measurement configuration: in (**a**,**b**) two views with $N = 20$ slot antennas are deployed over a hemispherical cup which hosts the breast under test, in (**c**) picture of hemispherical cup in absence of the breast.

Downstream the optimization process, each antenna has size of 18 mm × 11 mm, so that overall N = 20 antennas can easily be arranged over the cup. The positions (sketched in Figure 1a,b) are chosen so to have a good coverage of the breast during the irradiation stage. Usually, in medical applications as breast imaging, to improve the coupling between the antenna and the breast under investigation, a coupling medium is adopted. Typically, this requires to adopt a liquid matching material where the both antennas and breast are immersed. However, our system by adopting slot antennas that work in direct contact to the breast, both miniaturization and good coupling can be achieved without coupling media. Nevertheless, our system has the advantages that if a matching strategy is needed (i.e., a different antenna is employed), this can be be achieved by adopting a solid dielectric layer posed exactly in correspondence at the antennas' housing. Obviously, in the antenna optimization procedure, even the properties (i.e., dielectric and geometrical) of matching material must be taking into account [29].

3. Imaging Algorithm

The imaging problems consists in obtaining an image of the scene of the target under test from scattering measurements. The more simple measurement configuration is the monostatic one. Usually, a single antenna (i.e., transmitting and receiving) is used that moves around the target in order to realize a virtual array. Differently, our system based on multistatic configuration. Hence, while one antenna is transmitting, the field data are collected over the whole set of deployed antennas. Then, the process is repeated for each antenna. According, for each single frequency a total of N^2 measurements are performed.

To perform the reconstructions we first need to establish the math model whose inversion is actually the reconstruction process. To this end, we refer to the following equation

$$S(\omega, \underline{r}_{on}, \underline{r}_{om}) = S_{nm}(\omega) = (j\omega/2\pi v)\tilde{P}(\omega) \int_D \frac{\exp\left[\frac{-j\omega}{v}(|\underline{r}_{on} - \underline{r}| + |\underline{r}_{om} - \underline{r}|)\right]}{|\underline{r}_{on} - \underline{r}||\underline{r}_{om} - \underline{r}|} \chi(\underline{r}) d\underline{r}, \quad (1)$$

where $S_{nm}(\omega)$ is the scattering measurement at the angular frequency ω when the m-th antenna acts as transmitter and the n-th one as receiver, D is the spatial region under investigation and v the background medium propagation speed. Moreover, $\tilde{P}(\omega) = H_r(\omega)P(\omega)H_t(\omega)$, where $H_r(\omega)$ and $H_t(\omega)$ represent the receiving and transmitting antenna frequency responses and $P(\omega)$ the Fourier spectrum of the transmitted pulse. Finally, $\chi(\underline{r})$ is the so-called contrast function which describes the target in terms of its dielectric relative difference with respect to the background medium.

Equation (1) relies on different assumptions. First, the scattering phenomenon is considered being linear by invoking the Born approximation [30,31]. The cost to pay, as argued in the introduction, is that the corresponding images allow only to highlight and locate strong inhomogeneities. Also, the propagation speed is assumed known and constant. Although linearization hardly works and constant velocity clearly does not comply with the typical inhomogeneous and unknown tissue distribution of the breast, these assumptions are actually behind any radar imaging approach.

At this point it is worth taking into account that the breast properties are patient depend, then are unknown. However, since the antennas work near the breast, the behaviour of the antennas are unknown too. This implies that in (1), $H_r(\omega), H_t(\omega)$ and $P(\omega)$ are unknown as well. Therefore, classical beam-forming algorithms can experience a significant performance degradation. To see this, the indicator BF reported below can be useful (see [20])

$$I_{BF}(\underline{r}) = \left| \int_\Omega \sum_{n=1}^{N} \sum_{m=1}^{N} S_{nm}(\omega) \exp\left[j\omega\tau_{nm}(\underline{r})\right] d\omega \right|^2, \tag{2}$$

where Ω is the frequency band, $\underline{r}$ is the focusing point and $\tau_{nm}(\underline{r}) = (|\underline{r}_{on} - \underline{r}| + |\underline{r}_{om} - \underline{r}|)/v$ the set of delays to achieve focusing. Since $H_r(\omega), H_t(\omega)$ and $P(\omega)$ shape the data frequency behaviour, their precise estimations is essential for successfully focusing. This, however, is difficult due to the close proximity set up. It must be emphasized that this drawback arises because the frequency data are coherently summed. To mitigate this problem an incoherent beam-forming (IBF) scheme is proposed. The related indicator is reported below,

$$I_{IBF}(\underline{r}) = \int_\Omega \left| \sum_{n=1}^{N} \sum_{m=1}^{N} S_{nm}(\omega) \exp\left[j\omega\tau_{nm}(\underline{r})\right] \right|^2 d\omega, \tag{3}$$

where the basic difference with respect to (2) is clearly that data are summed in amplitude along the frequency domain. From the achievable performance point of view, in [20] it was shown that, for a monostatic configuration, the main difference occurs in the side-lobe of the point-spread function, hence the achievable resolution are practically the same in both cases. The same is expected to hold for the considered multistatic configuration.

4. Some Numerical Results

The proposed incoherent strategy is validate with some numerical experiments. All results refers to the case the breast is composed by only two tissue: skin and fat. In order to emulate the uncertainties of breast tissues, both skin and fat features are randomly perturbed 10% with respect to the nominal values mentioned above. The tumour is represented by a spherical inhomogeneity with diameter of 10 mm or 5 mm and three cases corresponding to different positions inside the breast are considered. Finally, in the imaging procedure process the background medium velocity is choose equal to the one in the fat tissue at frequency of 5 GHz. The reconstruction results are reported in Figure 2. As can be seen, in all the scenarios considered, the tumour is always detected and well localized.

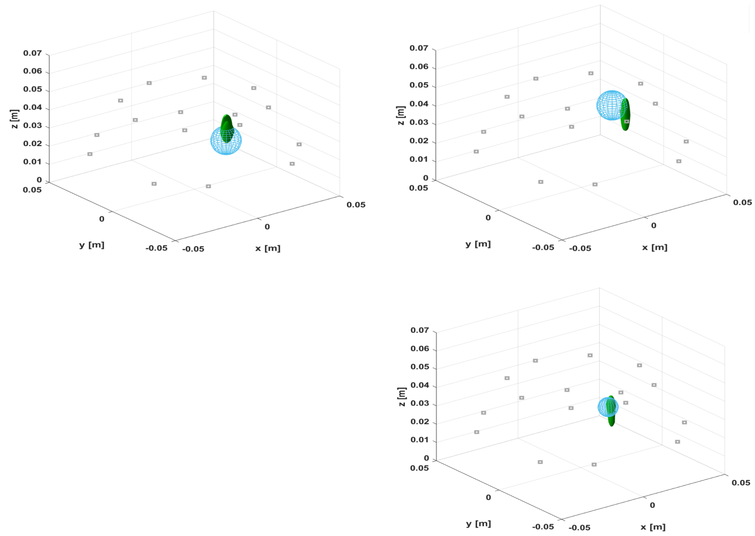

Figure 2. Reconstructions obtained via (3). The blue spheres represent the actual tumours, the green patches the corresponding reconstructions and the white squares denote the antenna positions. The reconstructions on the first row refers to the tumour's radius of 10 mm whereas the reconstruction on the second row to the radius of 5 mm.

5. Conclusions

Microwave breast imaging is a promising diagnostic method that can be used to help standard imaging modalities. Nonetheless, to the successful, MBI requires to properly address a number of issues. In this contribution, we just spotted the light on the one related to the antenna's response. The antenna's response has to be accounted for during the imaging stage since it "shapes" the actually received pulse and, above all, modifies the overall round-trip delay. This requires that it must be estimated so to allow to be put in or compensated for. Because in diagnostics the antennas are generally deployed near, or almost always in contact, to the target under test (in this paper we considered the breast), the antenna couples with the unknown target. As a consequence, its response deviates from its free-space counterpart. Therefore, while the latter can be easily measured/estimated, it shows to be of less practical use in diagnostics. This inconvenient is exacerbated by the patient to patient tissue changes. In this paper, we have shown that the knowledge of the antenna's frequency response is not necessarily required. Indeed, we have shown that the related issue can completely be overcome by adopting the incoherent strategy. Basically it consists in processing each frequency data separately and then realize the image. Each single-frequency image is summed (in amplitude) with the other performing the incoherent scheme. The numerical results has been confirmed the goodness of the proposed method. This encourage to consider a more numerical realistic breasts. Finally, the effectiveness and validity of the proposed incoherent strategy must be confirmed toward experimental and realistic scenarios.

Author Contributions: Conceptualization, B.B. and R.S.; methodology, A.C., A.D., R.S. and A.C.; software, A.C. and A.D.; validation, A.C. and A.D.; formal analysis, A.C. and A.D.; writing—original draft preparation, A.C., A.D. and R.S.; supervision, R.S. All authors have read and agreed to the published version of the manuscript.

Funding: This research was funded by B&B under the contract "ATTIVITA' DI RICERCA E PROGETTAZIONE DI DISPOSITIVI DI DETECTION A RADIOFREQUENZA PER DEVICE DI DIAGNOSTICA MEDICA PER IL SENO-RIFERIMENTO PROGETTO MIT MEDICAL DEVICE–AVVISO PUBBLICO PER IL SOSTEGNO ALLE MPMI CAMPANE CUP B17H22001730007".

Institutional Review Board Statement: Not applicable.

Informed Consent Statement: Not applicable.

Data Availability Statement: Data are contained within the article.

Acknowledgments: Antonio Cuccaro acknowledges the MUR (Ministero dell'Università e della Ricerca), Italy, as part of Project PNRR "AGE-IT" (Ageing well in an ageing society) a valere sull'avviso Partenariati Estesi (PE) del MUR.

Conflicts of Interest: The authors declare no conflicts of interest.

References

1. Ferlay, J.; Soerjomataram, I.; Eser, R.D.S.; Mathers, C.; Rebelo, M.; Parkin, D.M.; Forman, D.; Bray, F. Cancer incidence and mortality worldwide: Sources, methods and major patterns in GLOBOCAN 2012. *Int. J. Cancer* **2015**, *136*, E359–E386. [CrossRef]
2. Levi, F.; Bosetti, C.; Lucchini, F.; Negri, E.; La Vecchia, C. Monitoring the decrease in breast cancer mortality in Europe. *Eur. J. Cancer Prev.* **2005**, *14*, 497–502. [CrossRef] [PubMed]
3. Myers, E.R.; Moorman, P.; Gierisch, J.M.; Havrilesky, L.J.; Grimm, L.J.; Ghate, S.; Davidson, B.; Mongtomery, B.R.C.; Crowley, M.J.; McCrory, D.C.; et al. Benefits and Harms of Breast Cancer Screening: A Systematic Review. *JAMA* **2015**, *314*, 1615–1634. [CrossRef] [PubMed]
4. Siegel, R.L.; Miller, K.D.; Jemal, A. Cancer statistics. *CA Cancer J. Clin.* **2016**, *66*, 7–30. [CrossRef] [PubMed]
5. Preece, A.W.; Craddock, I.; Shere, M.; Jones, L.; Winton, H.L. Maria M4: Clinical evaluation of a prototype ultrawideband radar scanner for breast cancer detection. *J. Med. Imaging* **2016**, *3*, 033502-1–033502-7. [CrossRef]
6. Meaney, P.M.; Fanning, M.W.; Li, D.; Poplack, S.P.; Paulsen, K.D. A clinical prototype for active microwave imaging of the breast. *IEEE Trans. Microw. Theory Tech.* **2000**, *48*, 1841–1853.
7. O'Loughlin, D.; O'Halloran, M.; Moloney, B.M.; Glavin, M.; Jones, E.; Elahi, M.A. Microwave Breast Imaging: Clinical Advances and Remaining Challenges. *IEEE Trans. Biomed. Eng.* **2018**, *65*, 2580–2590. [CrossRef]
8. Kwon, S.; Lee, S. Recent Advances in Microwave Imaging for Breast Cancer Detection. *Int. J. Biomed. Imaging* **2016**, 5054–5912. [CrossRef]
9. Larsen, L.; Jacobi, J. Microwaves offer promise as imaging modality. *Diagn. Imaging* **1982**, *11*, 44–47.
10. Nikolova, N.K. Microwave imaging for breast cancer. *IEEE Microw. Mag.* **2011**, *12*, 78–94. [CrossRef]
11. Golnabi, A.H.; Meaney, P.M.; Epstein, N.R.; Paulsen, K.D. Microwave imaging for breast cancer detection: Advances in three-dimensional image reconstruction. In Proceedings of the 2011 Annual International Conference of the IEEE Engineering in Medicine and Biology Society, Boston, MA, USA, 30 August–3 September 2011; pp. 5730–5733.
12. Wang, L. Early Diagnosis of Breast Cancer. *Sensors* **2017**, *17*, 1572. [CrossRef] [PubMed]
13. Donelli, M.; Craddock, I.; Gibbins, D.; Sarafianou, M. A three-dimensional time domain microwave imaging method for breast cancer detection based on an evolutionary algorithm. *Prog. Electromagn. Res. M* **2011**, *18*, 179–195. [CrossRef]
14. Isernia, T.; Pascazio, V.; Pierri, R. On the local minima in a tomographic imaging technique. *IEEE Trans. Geosci. Rem. Sens.* **2001**, *39*, 1596–1607. [CrossRef]
15. Chew, W.C. *Waves and Fields in Inhomogeneous Media*; IEEE Press: New York, NJ, USA, 1995.
16. Chen, J.; Yao, K.; Hudson, R. Source localization and beamforming. *IEEE Signal Process. Mag.* **2002**, *19*, 30–39. [CrossRef]
17. Hagness, S.C.; Taove, A.; Bridges, J.E. Two-dimensional FDTD analysis of a pulsed microwave confocal system for breast cancer detection: Fixed focus and antenna array sensors. *IEEE Trans. Biomed. Eng.* **1998**, *45*, 1470–1479. [CrossRef] [PubMed]
18. Lim, H.; Nhung, N.; Li, E.; Thang, N. Confocal microwave imaging for breast cancer detection: Delay-multiply-and-sum image reconstruction algorithm. *IEEE Trans. Biomed. Eng.* **2008**, *55*, 1697–1704.
19. Klemm, M.; Craddock, I.J.; Leendertz, J.A.; Preece, A.; Benjamin, R. Improved delay-and-sum beamforming algorithm for breast cancer detection. *Int. J. Ant. Propag.* **2008**. [CrossRef]
20. Solimene, R.; Cuccaro, A.; Ruvio, G.; Tapia, D.F.; Halloran, M.O. Beamforming and Holography Image Formation Methods: An Analytic Study. *Opt. Express* **2016**, *24*, 9077–9093 [CrossRef]
21. Ruvio, G.; Solimene, R.; Cuccaro, A.; Fiaschetti, G.; Fagan, A.J.; Cournane, S.; Cooke, J.; Ammann, M.J.; Tobon, J.; Browne, J.E. Multimodal Breast Phantoms for Microwave, Ultrasound, Mammography, Magnetic Resonance and Computed Tomography Imaging. *Sensors* **2020**, *20*, 2400. [CrossRef]
22. Ruvio, G.; Solimene, R.; D'Alterio, A.; Ammann, M.J.; Pierri, R. RF breast cancer detection employing a non-characterized vivaldi antenna and a MUSIC-like algorithm. *Int. J. RF Microw. Comput. Aided Eng.* **2013**, *23*, 598–609. [CrossRef]
23. Ruvio, G.; Cuccaro, A.; Solimene, R.; Brancaccio, A.; Basile, B.; Ammann, M.J. Microwave bone imaging: A preliminary scanning system for proof-of-concept. *IEEE Healthc. Technol. Lett.* **2016**, *3*, 218–221. [CrossRef] [PubMed]
24. Ruvio, G.; Solimene, R.; Cuccaro, A.; Ammann, M.J. Comparison of Non-Coherent Linear Breast Cancer Detection Algorithms Applied to a 2-D Numerical Breast Model. *IEEE Antennas Wirel. Propag. Lett.* **2013**, *41*, 853–856. [CrossRef]
25. Ruvio, G.; Solimene, R.; Cuccaro, A.; Gaetano, D.; Browne, J.E.; Amman, M.J. Breast cancer detection using interferometric MUSIC: Experimental and numerical assessment. *Med. Phys.* **2014**, *41*, 102101–102111. [CrossRef] [PubMed]
26. Solimene, R.; Basile, B.; Browne, J.; Cuccaro, A.; Dell'Aversano, A.; Ruvio, G. An incoherent radar imaging system for medical applications. In Proceedings of the 2021 IEEE Conference on Antenna Measurements and Applications (CAMA), Antibes Juan-les-Pins, France, 15–17 November 2021.

27. Cuccaro, A.; Dell'Aversano, A.; Ruvio, G.; Browne, J.E.; Solimene, R. Incoherent radar imaging for breast cancer detection and experimental validation against 3D multimodal breast phantoms. *J. Imaging* **2019**, *7*, 23. [CrossRef]
28. Gabriel, S.; Lau, R.W.; Gabriel, C. Dielectric properties of biological tissue: III. Parametric models for the dielectric spectrum of tissues. *Phys. Med. Biol.* **1996**, 41, 2271–2293. [CrossRef]
29. Costanzo, S.; Cuccaro, A.; Dell'Aversano, A.; Buonanno, G.; Solimene, R. Microwave Biomedical Sensors with Stable Response: Basic Idea and Preliminary Numerical Assessments for Blood Glucose Monitoring. *IEEE Access* **2023**, *11*, 99058–99069. [CrossRef]
30. Marengo, E.A.; Galagarza, E.S.; Solimene, R. Data-driven linearizing approach in inverse scattering. *J. Opt. Spc. Am. A* **2017**, *34*, 1561–1576. [CrossRef]
31. Solimene, R.; Buonanno, A.; Soldovieri, F.; Pierri, R. Physical optics imaging of 3-D PEC objects: Vector and multipolarized approaches. *IEEE Trans. Geosci. Rem. Sens.* **2009** *48*, 1799–1808. [CrossRef]